MOLECULAR ECOLOGY

Origin and demographic history of the endemic Taiwanese spruce (Picea morrisonicola)

Journal:	*Molecular Ecology*
Manuscript ID:	MEC-13-0253
Manuscript Type:	Original Article
Date Submitted by the Author:	13-Mar-2013
Complete List of Authors:	Bodare, Sofia; Uppsala University, Ecology end Genetics Stocks, Michael; Uppsala University, Ecology end Genetics Yang, Jeng-Chuann; Taiwan Forestry Research Institute, Division of Botanical Garden Lascoux, Martin; Uppsala University, Ecology and Genetics
Keywords:	Climate Change, Conservation Genetics, Population Dynamics, Speciation

Origin and demographic history of the endemic Taiwanese spruce (*Picea morrisonicola*)

Sofia Bodare[1‡], Michael Stocks[1‡], Jeng-Chuann Yang[2], Martin Lascoux[1#]

1 Department of Ecology and Genetics
Evolutionary Biology Centre
Uppsala University, Uppsala Sweden

2 Botanical Garden Division,
Taiwan Forestry Research Institute, Taipei, Taiwan

‡These authors contributed equally to this work.

Author for correspondence: Martin.Lascoux@ebc.uu.se

Keywords: *Picea morrisonicola*, nucleotide diversity, Taiwan, Quaternary, bottleneck, ABC, power

Abstract

Taiwan spruce (*Picea morrisonicola*) is a vulnerable conifer species endemic to the island of Taiwan. A warming climate and competition from subtropical tree species has limited the range of Taiwan spruce to the higher altitudes of the island. Using seeds sampled from a population in central Taiwan, 15 nuclear loci were sequenced in order to measure genetic variation and to assess the long-term genetic stability of the species. Genetic diversity is low and comparable to other spruce species with limited ranges such as *P. breweriana*, *P. chihuahuana* and *P. schrenkiana*. Importantly, analysis using Approximate Bayesian Computation (ABC) shows evidence for a drastic decline in the effective population size approximately 0.3-0.5 million years ago. We used simulations to show that this is unlikely to be a false positive result due to the limited sample used here. To investigate the phylogenetic origin of Taiwan spruce, additional sequencing was performed in the Chinese spruce *P. wilsonii* and combined with previously published data for three other mainland China species, *P. purpurea, P. likiangensis* and *P. schrenkiana*. Analysis of population structure revealed that P. morrisonicola clusters most closely with P. wilsonii and coalescent analyses using MIMAR dated the split to 4-8 million years ago, coincidental to the formation of Taiwan. Considering the population decrease that occurred after the split, however, led to a much more recent origin.

Introduction

In the face of global warming many species will either have to adapt to the new conditions, migrate to new suitable areas or go extinct. For some species global warming will be a greater challenge than for others. For example, species confined to islands or other isolated geographic areas will have limited opportunities to migrate to new areas. The very same species will, due to their restricted geographic distribution range, often have small effective population sizes and therefore have a limited ability to adapt to the new climate. An example of such a species is the Taiwan endemic (*Picea morrisonicola* Hay.), which occurs in a very restricted natural distribution range and is listed as "Vulnerable" by the International Union for Conservation of Nature and Natural Resources (IUCN) (Conifer specialist group 2000) due to overexploitation from logging.

As the southernmost spruce species (The Gymnosperm Database, http://conifers.org/pi/Picea.php), the Taiwan spruce is subjected to very different climatic pressures than its mainland or boreal relatives. Pollen analyses indicate that "boreal" species, such as *Tsuga chinensis*, *Abies kawakamii* and *Picea morrisonicola* occupied lowland areas of central Taiwan between 60,000 – 50,000 years ago when the climate was cooler than today (Tsukada 1966). However, the climate in Taiwan has steadily warmed over the last 60,000 years and the increasing temperature has meant that expanding populations of both cool-temperate and subtropical species have pushed *P. morrisonicola* into the higher altitudes of the island (Tsukada 1966). As such, *P. morrisonicola* represents an example of a species that has already had to adapt to a warming climate, intense competition and a restricted area into which to escape. It is therefore of interest to study how these circumstances have shaped present and historical levels of genetic variation so that we can understand the impact of climate change. A great deal can therefore be learned by studying the impact that these climate shifts have had on genetic variation.

Taiwan provides in itself an intriguing setting for population genetic studies. Proto-Taiwan was formed by a collision of the Eurasian and the Philippine Sea plates likely about 9 million years ago (mya), although estimates vary. This was followed by a period of tectonic and volcanic activity before it acquired its modern shape (Sibuet & Hsu 1997, 2004). Since then, it has intermittently been connected to mainland China via a land bridge during glacial maxima, enabling it to serve as a refugium. The floristic relationship between Taiwan and mainland China

is probably complex. While some studies have found close resemblance and recent speciation processes, 25% of Taiwan's vascular flora is endemic. Also, Taiwan has been found to harbor plant species of diverse origins, from geographically close areas in South-Eastern China to the more distant tropical Asia and even temperate regions (Chiang & Schaal 2006). Conifer species have been present on Taiwan for at least a few million years, as seen in *Taxus* (Gao *et al.* 2007) and *Taiwania* (Chou *et al.* 2011), which migrated 1.1 and 3.3 mya, respectively. Although several studies have been published on the floristic relationships between Taiwan and mainland China, a lot remains to be done.

There are therefore three main aims that can be pursued. Firstly, we sequenced 15 nuclear loci in 15 individuals from a natural population of *P. morrisonicola* to produce what is, to the best of our knowledge, the first population genetic study in Taiwan spruce that looks at multiple nuclear loci. Genetic data from chloroplast and mitochondrial DNA for *P. morrisonicola* have previously only focused on phylogenetic or comparative studies covering the genus *Picea* (Bouillé *et al.* 2010; Ran *et al.* 2006) or the family Pinaceae (Lin *et al.* 2010). Using this population genetic dataset we can therefore investigate whether Taiwan spruce harbors similar levels of genetic diversity to other spruce species with similarly restricted distributions.

Secondly, by capturing within-species genetic diversity, we assess the impact that a changing climate has had on the effective population size through time by testing a null model of constant effective population size against alternative demographic models. Our population genetic approach in this study means that the sampling of multiple independent loci is more informative about the ancestral process in comparison to sampling more individuals. However, given that the extent of sampling does impact the ability to distinguish between competing demographic models, for example very recent population growth (e.g. Keinan & Clark 2012), we simulate datasets under a number of different models and assess the power and false positive rate of model choice in ABC for a sample of our size.

Thirdly, we compare sequence data for a subset of these genes in four spruce species from mainland China, *P. likiangensis*, *P. purpurea*, *P. schrenkiana* and *P. wilsonii*, which we had already sequenced previously (Li *et al.* 2010). These species represent the main clades from which *P. morrisonicola* could derive (Ran et al. 2006). In total, twelve Asian spruce species have been assigned to two clusters, where *P. morrisonicola* has a basal position within the *P. wilsonii/P. purpurea* clade. Furthermore, *P. morrisonicola* has been found to be a close relative

to *P. wilsonii* in a multi-locus study of the complete *Picea* genus (Jianquan Liu, pers. communication). Hence, these four species provide a basis for estimating divergence time and gene flow between *P. morrisonicola* and species from mainland China. Specifically, we use two complementary Bayesian methods, Approximate Bayesian Computation (ABC; Beaumont *et al.* 2002) and MIMAR (Becquet & Przeworski, 2007) to estimate parameters from between-species coalescent models. While both methods use coalescent simulations to model the ancestral process, each method has its own strengths and weaknesses. ABC compares summary statistics calculated from the data with those simulated under a model specified by the user. This method is approximate and assumes that the summary statistics chosen sufficiently capture aspects of the data relevant to the model. However, it is efficient and flexible to the extent that a number of different models can be tested and compared with one another. Contrastingly, MIMAR is a Markov Chain Monte Carlo method that estimates parameters under an Isolation-with-Migration (IM) model. Although, it is less time efficient than ABC, it has been shown to reliably estimate the parameters of an IM model under a number of simplifying assumptions (Becquet & Przeworski 2007; Becquet & Przeworski 2009). We therefore look to play to the strengths of each method by performing model choice in ABC and comparing parameter estimates from both MIMAR and ABC to strengthen our conclusions. We supplement these approaches with the clustering algorithm implemented in *Structure* (Pritchard *et al.* 2000) to assess the relationship of this endemic species with those from mainland China.

Material and Methods

Data collection and sequence editing

Seeds were collected from 15 different trees growing in the main distribution area of *Picea morrisonicola* (Fig. 1 & Supplementary Table 1). Relief data for Taiwan were obtained from Global Land 1-km Base Elevation Project (GLOBE Task Team *et al.*, 1999). Fifteen loci (4CL, GI2, GI4, GI6, PCH, SE1107, SE1390, SE1464, SE1427, SE6, EBS, M002, SB16, SB29, SB62) were used for sequencing. Nine loci were amplified using primers designed in previous studies (4CL, PCH, M002 Li *et al.*, 2010; EBS, SE1390: Heuertz *et al.* 2006; SB16, SB29, SB62: Chen *et al.* 2010) whilst four loci were amplified using loci designed from an expressed sequence tag (EST) survey of Norway spruce individuals (SE1107, SE1464, SE1427, SE6: Ivanissevich & Morgante, unpublished data, but see also Heuertz *et al.* 2006). The primers for loci GI2, GI4 and

GI6 were designed based on the cDNA for the circadian clock gene *Gigantea* (Gyllenstrand *et al.*, *in prep.*). The loci were chosen to be single or low copy genes. DNA was extracted from the haploid megagametophyte tissue of one seed per individual using Qiagen plant DNA extraction kit. All PCR reactions were made using high-fidelity proof-reading Phusion Enzyme in HF buffer and according to the instructions of the manufacturer. The PCR products were purified using Exo-SAP IT and sequenced on ABI3730 at Macrogen Korea using both forward and reverse primers and in the rare cases where quality was not satisfactory we performed additional sequence reactions. Sequences were base-called, visually inspected and edited using the software suite Phred, Phrap and Consed (Ewing *et al.* 1998; Ewing and Green 1998; Gordon *et al.* 1998). Only sequences with a Phred quality score above 20 were retained for further analysis. For the between-species analyses, 8 loci (4CL, EBS, M002, PCH, SB16, SB29, SB62, SE1390) for *P. likiangensis*, *P. purpurea*, *P. schrenkiana* and *P. wilsonii* were taken from a previous study (Li *et al.* 2010) for the structure analysis, with a further 6 loci sequenced in *P. wilsonii* (GI2, GI4, GI6, SE6, SE1107, SE1464) to supplement the coalescent based analysis. Seeds were sampled from 4, 6, 6 and 15 populations of *P. schrenkiana*, *P. wilsonii*, *P. purpurea* and *P. likiangensis*, respectively, with a total of 23-80 individuals per species. All sequences have been archived in DRYAD with accession numbers XXXXX). Summary statistics were calculated using the program EggLib (de Mita & Siol 2012), with the significance of Tajima's D and Fay & Wu's H calculated using the *libsequence* module *compute* (Thornton 2003).

Genetic structure

To analyze the relationship of *P. morrisonicola* with the four mainland species (*P. likiangensis*, *P. purpurea*, *P. schrenkiana* and *P. wilsonii*), we first used the software *Structure v. 2. 3. 2* (Pritchard *et al.* 2000). It uses unlinked markers to find the optimal number of clusters (*K*) in a data set. 192 single nucleotide polymorphisms (SNP) were recorded over the 10 loci where data was available for all five species. Since markers that are extremely close together can interfere with the analysis, only SNPs that were situated at least 50 bp apart were retained, resulting in a final data set of 62 SNPs from 8 loci. In total, 173 individuals from the five species were included in this analysis, and the number of successfully sequenced individuals per locus and species were 24-58 in *P. likiangensis*, 5-14 in *P. morrisonicola*, 10-22 in *P. purpurea*, 11-20 in *P. schrenkiana* and 12-29 in *P. wilsonii*.

The admixture model with correlated allele frequencies was used, and information on population identity was included to enable the LOCPRIOR function. The results were also double-checked with the independent frequency model. Burnin length was set to 10,000 and the number of iterations after burnin was 100,000. *Structure* was set to evaluate *K*=1 through *K*=10, and the results from 10 runs of each value of *K* were averaged. To find the optimal *K*, the average estimated posterior probabilities of data were considered, as well as the summary plots and ΔK calculated as in Evanno *et al.* (2005).

Estimate of divergence between *P. morrisonicola* and *P. wilsonii* using MIMAR

Based on the results from the *Structure* analysis that *P. wilsonii* is the closest relative to *P. morrisonicola* among the four species studied, we estimated divergence between *P. morrisonicola* and *P. wilsonii* with MIMAR (Becquet & Przeworski 2007; Becquet and Przeworski 2009). MIMAR is a program that estimates five demographic parameters in an isolation-migration model with two populations: the population mutation rate per base pair per generation for the ancestral population (θ_A) and for the two descendant populations (θ_1 and θ_2), the time in generations since the split (T) and the symmetrical migration rate (m). The data are summarized by dividing the segregating sites into categories depending on their presence or absence in each of the populations. Then genealogies are simulated and subsequently accepted or rejected by a Markov Chain Monte Carlo algorithm to give posterior distributions of the parameters of interest.

Outgroup sequences were taken from *Picea breweriana* (Chen *et al.* 2010) in most cases and from *Picea schrenkiana* (Li *et al.* 2010) in the few loci where *P. breweriana* sequences were ambiguous or missing. The population mutation rate was set to 2.5×10^{-8} per site *per generation*, which is taken from the mean value of the upper and lower bounds of the estimate of the mutation rate per site and per year in the genus *Pinus* ($0.7\text{-}1.31\times10^{-9}$ site per year; Willyard *et al.* 2007) and *Picea* (substitution rate of $0.6\text{-}1.1\times10^{-9}$ site per year; Chen *et al.*, 2012) and adjusted to an assumed generation time comprised between 25 and 50 years (Brown *et al.* 2004; Petit & Hampe 2006). However, it should be noted that estimated mutation rates vary between species in the literature, and that a study on *Picea* found a somewhat lower mutation rate, although based on a much smaller number of loci (Bouillé & Bousquet 2005). In general, estimates of divergence time are sensitive to the given mutation rate and generation time and

should therefore be interpreted with caution. After exploratory runs, the following prior bounds were chosen: θ_1 (0, 0.007), θ_2 (0, 0.002), θ_A (0, 0.015), T (0, 500 000) and ln(m) (-5, 1). The number of genealogies generated per step was increased to 50 since it was found to improve the acceptance rate considerably. 20 million steps were performed after a burnin of 2 million steps. The final analysis was done two times using different random seeds.

MIMARgof, a goodness of fit test, which is included in the MIMAR package, was performed on the results. It generates samples of summary statistics given the parameters estimated by MIMAR, and compares the distribution of the simulated samples with the observed values from the data set. This allows one to test whether the observed value falls within the range of the simulated values.

Within-species ABC models

To understand the demographic history of *P. morrisonicola*, four simple within-species demographic models (Fig. 2) were fit to the observed data. Three of these were chosen to reflect the observed positive Tajima's D value (0.28), which suggests a slight excess of intermediate variants. The population scaled mutation and recombination rates are consistent across each of the models and are defined as $\theta=4N_e\mu$ and $\rho=4N_er$, respectively, where N_e is the effective population size, μ is the mutation rate per site and *r* is the recombination frequency. Changes in the effective population size for the instantaneous bottleneck and population decline models are given by the parameter α, which represents the relative effective population size. For the instantaneous bottleneck model, a population of effective population size N_e experiences at *t* coalescent time units in the past a reduction in effective population size to αN_e, that persists for 0.2 coalescent time units (where coalescent time units are measured in $4N_e$ generations), before returning to the original effective population size. We choose to fix the duration of the bottleneck as the severity and duration parameters are confounded in the model. In the population decline model, the effective population size changes from αN_e to N_e t coalescent time units in the past. A structured population model was also considered where two populations experience a symmetrical population scaled migration rate $M=4N_em$, where *m* is the instantaneous migration rate. These models were compared with each other and against a 'null' constant effective population size model consisting of just the two parameters θ and ρ. The priors for the model parameters were uniformly distributed as θ:(0, 0.01), ρ:(0, 0.02), t:(0, 1.5),

M:(0.05, 1), α:(1, 1.5). A total of 11 summary statistics (Supplementary Table 2) were chosen to simulate parameters for each model using the above prior distributions.

Between-species ABC models

MIMAR implements a split model for *P. wilsonii* and *P. morrisonicola* with and without migration but assumes that effective population sizes remain constant through time and this could lead to problems inferring the correct divergence time. To test the robustness of the results obtained with MIMAR we therefore used ABC to compare the simple split model evaluated in MIMAR with more complex demographic models. Four between-species coalescent models were set-up based on a simple split model (Fig. 3). In the simplest scenario an ancestral population of effective population size N_e split into two populations t coalescent time units in the past (measured in $4N_e$ generations). Due to the low diversity and positive Tajima's D in *P. morrisonicola*, we tested models that allow the effective population size of *P. morrisonicola* to vary. Two such scenarios are considered, an instant change model under which the effective population size of *P. morrisonicola* is reduced at divergence time (IC_m), and another where the decline in effective population size is delayed until some time point between divergence time and the present day (D_m). A model was also considered where the effective population sizes of both descendant populations went through an instantaneous change at divergence time (IC_{mw}), and another similar model but with an additional decline in the effective population size of *P. morrisonicola* after divergence (IC_{mw}+D_m). A simple split model was also considered where the effective population size remains constant throughout the coalescent process but this model received such low support in the model choice step that it was not considered further (data not shown).

Each model is parameterized by the population scaled mutation and recombination rates ($\theta=4N_e\mu$ and $\rho=4N_e r$, respectively, where μ is the mutation rate and r is the recombination frequency). Changes in the effective population size (α, α_m, α_w, α_{m0} and α_{m1}) are estimated relative to N_e and the time since population divergence (t_1) or a decline in *P. morrisonicola* (t_0) are estimated in coalescent time units (measured in $4N_e$ generations). A set of 29 summary statistics was calculated when simulating parameters under each of the models (Supplementary Table 2). The joint site frequency spectrum is the basic information on which the inference is based and can be summarized in various ways. We used Wakeley and Hey (1997) summary statistics as well as other summary statistics that were shown to be informative in other studies

(e.g. Clotault *et al.* 2012; Hickerson *et al.* 2006; Li *et al.* 2012). The priors were uniformly distributed with bounds θ:(0, 0.01), ρ:(0, 0.02), α, α_m, α_w, α_{m0}, α_{m1}:(0, 1.5) and t_1 ,t_1:(0, 1.5).

ABC parameter estimation, model choice and posterior predictive simulations

For each model, 10^6 simulations were performed and parameter estimation was performed using the Approximate Bayesian Computation method of Beaumont *et al.* (2002) with log transformation of parameters and a tolerance of 0.001. Model choice was performed according to the method implemented in Fagundes *et al.* (2007), with Bayes Factors calculated as the ratio of the marginal likelihoods of the competing models, $p(y|M_1)/p(y|M_0)$. A Bayes factor of 3 was considered high enough to reject model M_0 in favor of model M_1 (Kass & Raftery 1995). For the most probable models of the within and between species analyses, 1000 parameter values were sampled from the posterior predictive distribution and used to simulate summary statistics for comparison with the observed data. To assess the power and false positive rate of ABC model choice, 100 simulated datasets were generated for each of the models. Each dataset was simulated with the same number of samples and loci as that in the observed data. Model choice was then performed on each of the simulated datasets to establish the power and the false positive rate of ABC. All ABC analyses, coalescent simulations and summary statistic calculations for the ABC analyses were performed using the package *EggLib* (de Mita & Siol 2012).

Results

Nucleotide diversity and basic summary statistics

Seven out of the 15 genes sequenced in *P. morrisonicola* were completely monomorphic. Both estimates of total nucleotide diversity, Watterson's theta (θ_W), and the average number of pairwise nucleotide differences (π), are low (Table 1). Averaged across loci, θ_W and π give values of 0.00147 and 0.00146 per base pair, respectively. This suggests that occurrences of low and intermediate frequency variants are in line with standard neutral expectations; however, six out of eight polymorphic loci show an excess of intermediate frequency variants (i.e. $\pi > \theta_W$). This is reflected by a positive value of 0.281 for Tajima's D when averaged across loci. An excess of intermediate variants is indicative of evolutionary processes whereby the time to coalescence of the remaining two lineages is longer than would be expected under a neutral

coalescent model of constant effective population size. Additionally, an excess of high frequency variants was indicated by negative values of the normalized (Z) and non-normalized (H) versions of Fay & Wu's H. Two loci (4CL and SE1427) show significant deviations in Fay & Wu's H (H) from a simple coalescent model of constant effective population without recombination. The locus SE1427 also exhibits a significant deviation of Tajima's D from standard neutral expectations.

Genetic structure

The between-species clustering analysis suggests that *K*=4 is the minimum number of clusters that captures the most important population structure (Fig. 4). Although *K*=5 has a slightly higher probability, the curve starts to plateau at *K*=4. At this level, all species except *P. purpurea* make up their own cluster (Fig. 5). Before that, at *K*=*3*, *P. morrisonicola* clusters with *P. wilsonii*, suggesting that *P. morrisonicola* derived from the latter or that the two species have a common ancestor. The admixed nature of *P. purpurea* is in line with expectations since *P. purpurea* has previously been found to be a hybrid species between *P. wilsonii* and *P. likiangensis* (Li *et al.* 2010). The ΔK calculation suggests *K*=2 to be optimal, in which *P. schrenkiana* forms a cluster of its own (Supplementary Table 3).

Estimate of divergence between *P. morrisonicola* and *P. wilsonii* using MIMAR

Results from the analysis are shown in Table 2 and Figure 6. *P. wilsonii* and *P. morrisonicola* were found to have split about 160,000 generations ago, translating into 4 mya if a generation time of 25 years is assumed (90% CI 2.8-5.5 mya) or 8 mya if a generation time of 50 years is assumed (90% CI 5.6-11 mya). A low migration rate of 0.35 individuals per generation was detected. The population mutation rate, θ_2, suggests that *P. morrisonicola* was founded by a population of size N_e=5000 individuals after the split, given $\mu=2.5\times10^{-8}$. The goodness-of-fit tests (Supplementary Figure 3) show a good fit for some of the summary statistics, such as Tajima's D and the number of shared polymorphisms and fixed differences. Other summary statistics, including the number of segregating sites within *P. wilsonii* and the π calculated within *P. morrisonicola* (Supplementary Table 6), show a significant departure suggesting that whilst the retained model fits the data well, it does not accommodate all aspects of the demography of the species.

Within-species ABC

Table 3 shows Bayes factors and model probabilities for the four within-species demographic models applied to *P. morrisonicola*. The population decline model has the strongest support of all the models considered with a posterior probability of 0.5241. Bayes factors calculated between the population decline model and each of the competing models gave values of 8.7, 1.5 and 4.3 for the constant effective population size, bottleneck and population structure models, respectively. Both the constant effective population size and structure models could be rejected in favor of the decline model, assuming a Bayes factor significance threshold of 3 (Kass & Raftery 1995). The bottleneck model cannot be rejected in favor of the population decline model. However, given that the Bayes factor favors a population decline we estimate parameters and perform posterior predictive simulations to assess the fit of this model to the data. Parameter values estimated under the population decline model are shown in Table 5 and Supplementary Table 4: *P. morrisonicola*'s effective population size declined from around 124,000 to 1,800 approximately 11,000 generations ago (assuming a per site and per generation mutation rate of 2.5×10^{-8}). Assuming a generation time of 25 and 50 years, this would date the decline at approximately 270,000 years ago and 537,000 years ago, respectively.

The posterior predictive simulations under the population decline model are given in Supplementary Figure 1. Tajima's D, haplotype diversity and the standard deviation of π fit the observed data well. The relative site frequency spectrum also fit the data well, although the distributions of θ_H and H indicate that there is a relative excess of high frequency derived variants in the observed data compared to the posterior predictive distributions.

Between-species ABC

Bayes factors and model probabilities for each of the four between-species models tested for *P. wilsonii* and *P. morrisonicola* are shown in Table 4. The delayed decline model (D_m) shows the highest model probability (0.4512), and has Bayes' factors of 2.3, 3.7 and 1.8 when compared to the IC_m, IC_{mw} and IC_{mw}+D_m models respectively. Neither the IC_m nor the IC_{mw}+D_m models can be rejected (assuming a significant Bayes factor of 3), so we estimated the parameters of the most probable model (D_m) and performed posterior predictive simulations to check the fit of the model to the data. Table 5 and Supplementary Table 5 show the parameters estimated under

the D_m model and indicate that *P. wilsonii* and *P. morrisonicola* split from an ancestral population with an effective size of 44,000 approximately 45,000 generations in the past (assuming a per site and per generation mutation rate of 2.5×10^{-8}). Within *P. morrisonicola* there was a reduction down to an effective population size of 4,200 at around 15,000 generations in the past. Assuming a generation time of 25 years, this gives a divergence time of 1.1 million years and a population decline occurring around 374,000 years ago. Assuming a generation time of 50 years would double these estimates to give a divergence time of 2.2 million years and a population decline occurring 0.75 million years ago.

Supplementary Figure 2 compares statistics from 1000 posterior predictive simulations with the observed values. Overall, the fit of the model to the data is good. There are a number of statistics, such as D1 and D, that do not fit the data very well. However, between-species statistics such as the Wakeley & Hey (1997) statistics and F_{ST} fit the data excellently, suggesting that estimates of divergence time under the D_m model should be robust.

Performance of ABC

There are two factors that need to be assessed due to the nature of the sampling. While population genetic studies typically require relatively few samples in order to capture important aspects of the genealogy, it is important to assess the power and false positive rate of the model choice step of ABC. Table 6 shows the power (proportion of datasets simulated under the decline model where the alternative model is correctly rejected) and the false positive rate (proportion of datasets simulated under an alternative model that are incorrectly rejected in favor of the decline model) for each of the alternative models of the within-species analysis. The power varies depending on the model of comparison, with 0.81, 0.3 and 0.95 for the constant N_e ,bottleneck and structure models respectively. The patterns produced by the bottleneck and decline models in contemporary modern data are expected to be similar and this is represented in the relatively low power allowed for rejecting the bottleneck model.

However, the false positive rate is relatively low. The constant N_e model has the highest false positive rate (0.07), with the bottleneck model (0.01) and the structure model (0) having rates lower than 5%. Given that the Bayes factor for the decline model was not always greater than 3, it is also of interest to look at the proportion of simulated datasets that yield a Bayes factor greater than that calculated from the observed data. Amongst the simulated datasets for the

406 constant N_e and structure models, there were no simulations for which the Bayes factor
407 exceeded the observed Bayes factor. For the bottleneck model, whilst the false positive rate
408 was still low, 12 % of the simulated datasets exceeded the observed Bayes factor.
409
410 **Discussion**
411
412 The range and distribution of Taiwan spruce has changed with its surrounding environment and
413 we aimed to look at the impact this change has had on genetic diversity. The foremost aims of
414 this population genetic study of the endemic Taiwan spruce were to: i) use patterns of sequence
415 diversity to look for historical changes in the effective population size, ii) identify the most likely
416 ancestor to *P. morrisonicola* and estimate the divergence time between these two species, and
417 iii) assess whether small samples can give reliable estimates of past demographics. We find
418 that *P. morrisonicola* is a species with a comparably low level of genetic diversity that went
419 through a steep decline in its effective population after splitting from P. wilsonii a few million
420 years ago.
421
422 *Genetic diversity and population demography*
423
424 Our survey of nucleotide diversity indicates that *P. morrisonicola* is among the less genetically
425 diverse spruce species with a nucleotide diversity of the same order of magnitude to that
426 observed in other marginal spruce species such as *P. breweriana* (π_s = 0.00200; Chen *et al.*
427 2010) which grows in small scattered montane populations in Northern California, or *P.*
428 *schrenkiana* (π_s = 0.00258; Li *et al.* 2010), found in slightly larger populations in the Tian Shan
429 mountain range at the north-western border of China. Similar results have also been found in
430 the Chihuahua spruce (*P. chihuahuana)*, which shares several features with *P. morrisonicola*. *P.*
431 *chihuahuana,* the southernmost spruce species of the American continent, is a relict species
432 endemic to the montane forests of Mexico. In this species very few chlorotypes and mitotypes
433 were found, and the diversity within populations was low (H = 0.415 for chlorotypes and H = 0
434 for mitotypes). Two distinct mitotypes were found, which is interpreted as suggesting that the
435 modern populations of this species originated from two ancestral populations in the near past
436 after a bottleneck (Jaramillo-Correa *et al.* 2006). Although evidence is still limited, low genetic
437 diversity might be common among peripheral populations in areas affected by glacial events.
438

We find evidence that the effective population size is smaller today than it was in the past. ABC analysis favors a within-species scenario where a 98.6% reduction in the effective population size occurs 11,000 generations in the past. This represents a drastic reduction in the effective population size, but may also explain why we are able to detect it. Due to the nature of our questions and the types of analyses used, our data collection focused more strongly on obtaining more loci as opposed to sampling more individuals. It is often the case that only limited samples are available and this can be a limiting factor in the estimation of range-wide genetic diversity, but may be much less problematic for inferences of past demographic events if a decent number of loci are available. Many of the most innovative studies carried out in Drosophila did not involve samples of more than 10-20 chromosomes (e.g. Thornton & Andolfatto, 2006; Singh *et al.* (in press)). Drosophila species generally have a very high level of genetic polymorphism and this may not extend to species that do not share the same degree of genetic polymorphism. It was therefore important to assess how good our inferences could be based on small samples in a less variable species. Accordingly, our simulations indicated that the power to correctly reject an alternative null model is low in small, genetically less diverse datasets. However, the false positive rate, measured as the proportion of datasets for which the null model is incorrectly rejected is also low. Overall, this means that while it is hard to reject a null hypothesis with a small sample size, a high Bayes factor is unlikely to be a false positive and instead represents a strong signal in the data.

Origin and relationship to Taiwan geological history

P. morrisonicola is a well defined and distinct species and its closest relative among the four spruce species examined is *P. wilsonii*, as shown by the *Structure* analysis. In contrast to the ancestry estimate plot and the calculated probabilities for each *K*, the ΔK analysis suggested only two clusters, in which *P. morrisonicola* would belong to the same cluster as all the other species examined except for the most geographically distant one, *P. schrenkiana*. However, ΔK is in some cases prone to underestimate the true *K*, e.g. when differentiation between populations is not strong (Waples & Gaggiotti 2006). Based on other studies in conifers and the large number of shared polymorphisms observed even between species on different continents (Chen *et al.* 2010), we may indeed not expect very strong population structure in this case. Instead, *K=4* can be justified from a biological point of view. Furthermore, our result suggesting that *P. wilsonii* and *P. morrisonicola* derive from the same common ancestor is corroborated by

the multi-locus phylogenetic analysis of the complete *Picea* genus that also place *P. morrisonicola* in the *P.wilsonii* clade (Jianquan Liu, pers. communication).

Assuming a generation time of 25-50 years, the split time between *P. wilsonii* and *P. morrisonicola* was estimated to be 4-8 million years by MIMAR and 1.1-2.2 million years by the D_m model of ABC. The latter estimates are close to those obtained in *Taxus* (Gao *et al.* 2007) and *Taiwania* (Chou *et al.* 2011), which migrated 1.1 and 3.3 mya, respectively, but the former is significantly larger. The discrepancy between the estimates of divergence for the two methods can in the most part be attributed to differences in the models. The Dm model delays a reduction in the effective population size for a few million years compared to the scenario modeled in MIMAR. Also, the IM model implemented in MIMAR allows for gene flow after divergence, which was not taken into account in the between-species ABC models. Both should lead to a longer divergence time in MIMAR. Additionally, even if these time estimates should be taken with a grain of salt due to their reliance on unwarranted assumptions about mutation rate and generation time, we note that they correspond well with either the time of formation of modern Taiwan, 4-5 mya, or the colonization by other conifer species, 1-3 mya.

Our data lends support to a scenario whereby *P. morrisonicola* evolved when migrants from the *P. wilsonii* clade reached Taiwan after the island was formed. This was during or just before the Pleistocene ice age began (2.8 mya) and although Taiwan was never under ice cover, temperatures were lower than today. During the Pleistocene repeated cycles of glacials and interglacials took place, whereby the population size of *P. morrisonicola* likely dropped considerably. Accordingly, a severe population decrease 0.37-0.74 mya was found by the Dm model of ABC. When temperatures started to rise again after the last glacial event, 11,800 years ago, *P. morrisonicola* may have begun to be confined to the higher altitudes of central Taiwan, resulting in the population distribution seen today.

Conservation

Pollen analyses have previously shown that *Picea* was far more prevalent between 50,000 and 60,000 years ago (Tsukada 1966). The reduction in the range of Taiwan spruce and its retreat to higher altitudes has coincided with a general increase in temperature in Taiwan. Taiwan spruce, therefore, represents an excellent study species for assessing the long-term impact of climate change on genetic diversity. Whilst it is difficult to attribute any genetic changes with

environmental shifts specifically, levels of genetic diversity are greatly reduced in Taiwan spruce compared to boreal spruce species and more in line with other spruce species with restricted distributions. Additionally, the data are consistent with the effective population size being considerably larger in the past, suggesting that environmental factors can have a big impact on genetic diversity within populations.

Temperatures are predicted to increase by between 0.9 and 2.7°C in the next 30 years compared to 1961-1990 average temperatures (Hsu *et al.* 2002). With studies correlating temperature with growth and demonstrating that a warmer January is negatively correlated with height growth (Guan *et al.* 2009, 2012), it is certainly of interest to consider how a further increase in temperature would affect Taiwan spruce in the long-term. Although *P. morrisonicola* has survived past climate fluctuations, the ability to adapt during future climate changes may not be preserved, for two reasons (Hermisson & Pennings 2005). Firstly, adaptations starting from standing genetic variation critically depend on the amount of genetic variation available, therefore the removal of standing genetic variation in Taiwan Spruce will reduce the probability that an adaptive allele is present in the current population. Secondly, the failure of Taiwan Spruce to recover to its pre-decline effective population size will limit the influx of new beneficial mutations into the population, a portion of which will inevitably be lost to genetic drift. However, these represent more long-term rather than short-term concerns as to the conservation status of Taiwan Spruce. It is worth noting that *P. morrisonicola* is relatively well protected in Taiwan today since logging of natural forests for commercial purposes was banned in 1991 and the remaining forests are still used for recreational and other less invasive purposes (World Forest Institute 2001).

Finally, from a conservation perspective, it would be of interest to assess the genetic diversity and structure in other locations across the distribution range. Since the present study focused on only one stand, some of the diversity may still be undiscovered. However, allozyme studies on a number of forest species suggest that central Taiwan is a major hotspot for within-species diversity (Lin 2001). Therefore, until data on species-wide diversity is available, conservation priority should be given to the populations of central Taiwan since this area is likely to harbor most of this species' genetic diversity.

Acknowledgements

Financial support was provided by The Swedish Research Council for Environmental, Agricultural Sciences and Spatial Planning, the European Commission (project EVOLTREE). SB was financed by a grant from the Swedish International Development Cooperation Agency (SIDA). ML would also like to thank the Chinese Academy of Sciences for a Visiting Professorship and Li Haipeng for his hospitality in Shanghai.

References

Beaumont MA, Zhang W, Balding DJ (2002) Approximate Bayesian computation in population genetics. *Genetics* **162**, 2025–2035.

Becquet C, Przeworski M (2007) A new approach to estimate parameters of speciation models with application to apes. *Genome Research*, **17**, 1505–1519.

Becquet C, Przeworski M (2009) Learning about modes of speciation by computational approaches. *Evolution*, **63**, 2547–2562.

Bouillé M, Bousquet J (2005) Trans-species shared polymorphisms at orthologous nuclear gene loci among distant species in the conifer *Picea* (Pinaceaea): implications for the long-term maintenance of genetic diversity in trees. *American Journal of Botany* **92**(1), 63-73.

Bouillé M, Senneville S, Bousquet J (2010) Discordant mtDNA and cpDNA phylogenies indicate geographic speciation and reticulation as driving factors for the diversification of the genus Picea. *Tree Genetics & Genomes*, **7**, 469-484.

Brown, G., Gill, G., Kuntz, R., Langley, C. & Neale, D. (2004). Nucleotide diversity and linkage disequilibrium in loblolly pine. *Proceedings of the National Academy of Sciences of the United States of America,* **101**, 15255-15260.

Chen J, Källman T, Gyllenstrand N, Lascoux M (2010) New insights on the speciation history and nucleotide diversity of three boreal spruce species and a Tertiary relict. *Heredity*, **104**, 3–

14.

Chen J, Uebbing S, Gyllenstrand N, Lagercrantz U, Lascoux M, Källman T (2012) Sequencing of the needle transcriptome from Norway spruce (*Picea abies* Karst L.) reveals lower substitution rates, but similar selective constraints in gymnosperms and angiosperms. *BMC Genomics*, **13**, 589.

Chiang T, Schaal B (2006) Phylogeography of plants in Taiwan and the Ryukyu archipelago *Taxon*, **55**, 31–41.

Chou Y-W, Thomas PI, Ge X-J, LePage BA, Wang C-N (2011) Refugia and phylogeography of Taiwania in East Asia. *Journal of Biogeography*, **38**, 1992-2005.

Clotault J, Thuillet AC ,Buiron M, De Mita S, Couderc M, Haussmann BIG, Mariac C, Vigouroux Y (2012). Evolutionary history of pearl millet (Pennisetum glaucum [L.] R. Br.) and selection on flowering genes since its domestication. *Molecular Biology and Evolution,* **29,** 1199–1212.

Conifer Specialist Group (2000) *Picea morrisonicola*. In: IUCN 2012. IUCN Red List of Threatened Species. Version 2012.1. <www.iucnredlist.org>. Downloaded on 05 September 2012.

de Mita S, Siol M (2012) EggLib: processing, analysis and simulation tools for population genetics and genomics. *BMC Genetics,* **13**, 27.

Evanno G, Regnaut S, Goudet J (2005) Detecting the number of clusters of individuals using the software STRUCTURE: a simulation study. *Molecular Ecology*, **14**, 2611–2620.

Ewing B, Hillier L, Wendl MC, Green P (1998) Base-calling of automated sequencer traces using phred. I. Accuracy assessment. *Genome Research*, **8**, 175-185.

Ewing B, Green P (1998) Base-calling of automated sequencer traces using phred. II. Error probabilities. *Genome Research,* **8**, 186-194.

Fagundes NJR, Ray N, Beaumont M, Neuenschwander S, Salzano FM, Bonatto SL, Excoffier L (2007) Statistical evaluation of alternative models of human evolution, *Proceedings of the*

National Academy of Sciences of the United States of America **104**, 17614–17619.

Gao LM, Möller M, Zhang X-M, Hollingsworth ML, Liu J, Mill RR, Gibby M, Li D-Z (2007) High variation and strong phylogeographic pattern among cpDNA haplotypes in Taxus wallichiana (Taxaceae) in China and North Vietnam. *Molecular Ecology,* **16**, 4684–4698.

GLOBE Task Team and others (Hastings, David A., Paula K. Dunbar, Gerald M. Elphingstone, Mark Bootz, Hiroshi Murakami, Hiroshi Maruyama, Hiroshi Masaharu, Peter Holland, John Payne, Nevin A. Bryant, Thomas L. Logan, J.-P. Muller, Gunter Schreier, and John S. MacDonald) (1999). *The Global Land One-kilometer Base Elevation (GLOBE) Digital Elevation Model, Version 1.0. National Oceanic and Atmospheric Administration, National Geophysical Data Center, 325 Broadway, Boulder, Colorado 80305-3328, U.S.A. Digital data base on the World Wide Web (URL: http://www.ngdc.noaa.gov/mgg/topo/globe.html) and CD-ROMs.*

Guan BT, Chung C-H, Lin S-T, Shen C-W (2009) Quantifying height growth and monthly growing degree days relationship of plantation Taiwan spruce. *Forest Ecology And Management*, **257**, 2270-2276.

Guan BT, Wright WE, Chung C-H, Chang S-T (2012). ENSO and PDO strongly influence Taiwan spruce height growth. *Forest Ecology And Management*, **267**, 50–57.

Gordon D, Abajian C, Green P (1998) Consed: A graphical tool for sequence finishing. *Genome Research,* **8**, 195-202.

Hermisson J, Pennings PS (2005) Soft sweeps: Molecular population genetics of adaptation from standing genetic variation. *Genetics,* **169**, 2335-2352.

Heuertz M, de Pauli E, Källman T, Larsson H, Jurman I, Morgante M, Lascoux M, Gyllenstrand N (2006) Multilocus patterns of nucleotide diversity, linkage disequilibrium and demographic history of Norway spruce [*Picea abies* (L.) Karst]. *Genetics,* **174**, 2095-2105.

Hickerson MJ, Dolman G, Moritz C (2006) Comparative phylogeographic summary statistics for testing simultaneous vicariance. *Molecular Ecology,* **15**, 209-223.

Hsu H-H, Chen C-T (2002). Observed and projected climate change in Taiwan. *Meteorology and Atmospheric Physics,* **79**, 87-104.

Jaramillo-Correa JP, Beaulieu F, Ledig T, Bousquet J (2006). Decoupled mitochondrial and chloroplast DNA population structure reveals Holocene collapse and population isolation in a threatened Mexican-endemic conifer. *Molecular Ecology,* **15**, 2787-2800.

Kass R, Raftery A (1995) Bayes Factors. *Journal of the American Statistical Association*, **90**, 773–795.

Li Y, Stocks M, Hemmilä S, Källman K, Zhu H, Zhou Y, Chen J, Liu J, Lascoux M (2010) Demographic histories of four spruce (*Picea*) species of the Qinghai-Tibetan Plateau and neighboring areas inferred from multiple nuclear loci. *Molecular Biology and Evolution,* **27**, 1001-1014.

Li S, Jakobsson M (2012) Estimating demographic parameters from large-scale population genomic data using Approximate Bayesian Computation. *BMC Genetics,* **13**, 22.

Lin C-P, Huang J-P, Wu C-S, Hsu C-Y, Chaw S-M (2010) Comparative chloroplast genomics reveals the evolution of Pinaceae genera and subfamilies. *Genome Biology and Evolution,* **2**, 504–517.

Lin, TP (2001) Allozyme variations in the Michelia formosana (Kanehira) Masamune (Magnoliaceae), and the inference of a glacial refugium in Taiwan. *Theoretical and Applied Genetics,* **102,** 450–457.

Petit RJ, Hampe A (2006) Some evolutionary consequences of being a tree. *Annual Review of Ecology, Evolution And Systematics*, **37**, 187–214.

Pritchard JK, Stephens M, Donnelly P (2000) Inference of population structure using multilocus genotype data. *Genetics,* **155**, 945–959.

Ran J-H, Wei X-X, Wang X-Q (2006) Molecular phylogeny and biogeography of *Picea*

(Pinaceae): Implications for phylogeographical studies using cytoplasmic haplotypes. *Molecular Phylogenetics and Evolution*, **41**, 405–419.

Sibuet JC, Hsu SK (1997) Geodynamics of the Taiwan arc-arc collision. *Tectonophysics,* **274**, 221–251.

Sibuet JC, Hsu SK (2004) How was Taiwan created? *Tectonophysics,* **379**, 159-181.

Singh ND, Jensen JD, Clark AG, Aquadro CF (2013) Inferences of Demography and Selection in an African Population of *D. melanogaster. Genetics*, **193**, 215-228.

Thornton K (2003) libsequence: a C++ class library for evolutionary genetic analysis. *Bioinformatics* **19**(17), 2325- 2327.

Thornton K, Andolfatto P (2006). Approximate Bayesian inference reveals evidence for a recent, severe bottleneck in a Netherlands population of *Drosophila melanogaster*. *Genetics*, *172*(3), 1607–1619.

Tsukada M (1966) Late Pleistocene Vegetation and Climate in Taiwan (Formosa). *Proceedings of the National Academy of Sciences of the United States of America,* **55**, 543-548.

Wakeley J, Hey J (1997) Estimating ancestral population parameters. *Genetics*, **145**, 847–855.

Waples RS, Gaggiotti O (2006). What is a population? An empirical evaluation of some genetic methods for identifying the number of gene pools and their degree of connectivity. *Molecular ecology* **15**, 1419–1439.

Willyard A, Syring J, Gernandt DS, Liston A, Cronn R (2007) Fossil calibration of molecular divergence infers a moderate mutation rate and recent radiations for *Pinus*. *Molecular Biology and Evolution* **24**(1), 90-101.

World Forest Institute (2001) Taiwan's Forest Sector. *WFI Market Brief Series,* 1-14.

710

Figure legends

Figure 1: Relief map of Taiwan showing the sampling locations (blue dots).

Figure 2: Within-population models of demography considered for ABC analysis, where N is the effective population size, α scales the effective population size during bottlenecks and declines, M is the population scaled mutation rate (4Nm) and t, t1 and t0 are the coalescent times of the decline and bottleneck events (measured in 4N generations).

Figure 3: Between-population models compared in the ABC analysis, where N is the effective population size, α, αm, αw, αm1 and αm0 scale the effective population sizes during bottlenecks and declines and t1 and t0 are the coalescent times of the divergence and decline events (measured in 4N generations).

Figure 4: Likelihood and standard deviation for each value of *K* in the *Structure* analysis on the five species *P. morrisonicola*, *P. likiangensis*, *P. purpurea*, *P. schrenkiana* and *P. wilsonii*.

Figure 5: Ancestry estimates from *Structure* for *K*=2 through *K*=10 in the five species *P. likiangensis* (P.l.), *P. purpurea* (P.p.), *P. schrenkiana* (P.s.), *P. wilsonii* (P.w.) and *P. morrisonicola* (P.m.). Each *K* is represented by the *Structure* run that rendered the highest likelihood and shows the individual's estimated proportion of membership to each cluster.

Data Accessibility

Data on sample locations, DNA sequences and input files used in MIMAR and *Structure*
are uploaded on DRYAD as entry doi:(...).

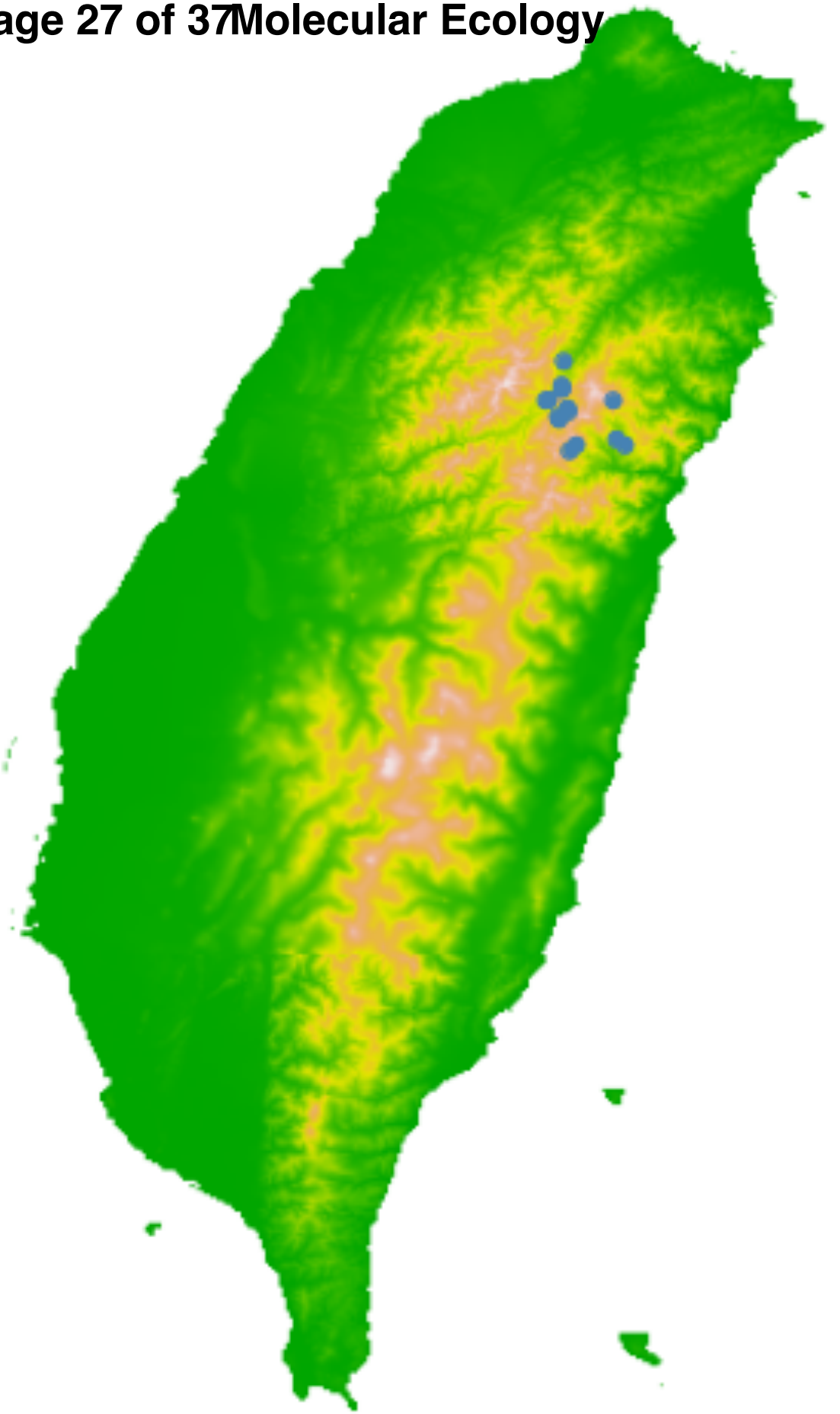

Constant Effective Population Size

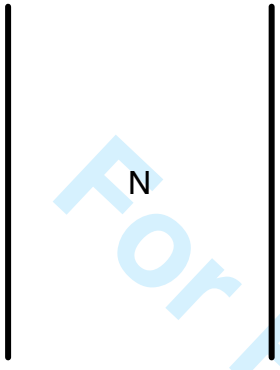

Bottleneck

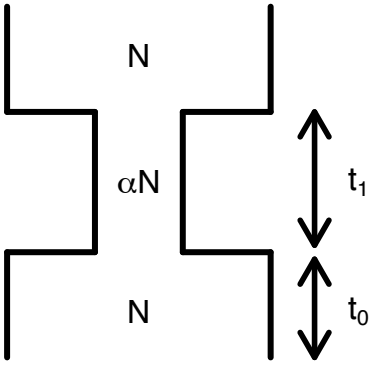

Population Structure

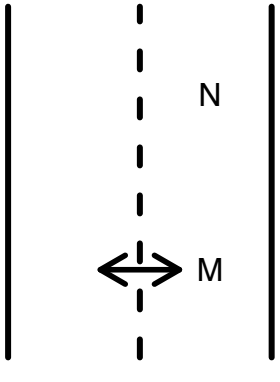

Decline

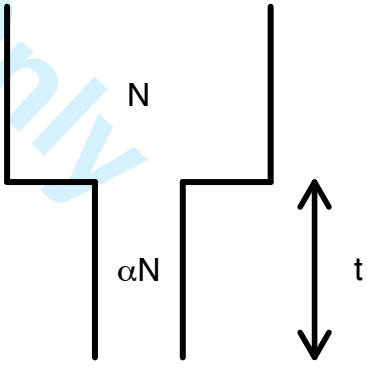

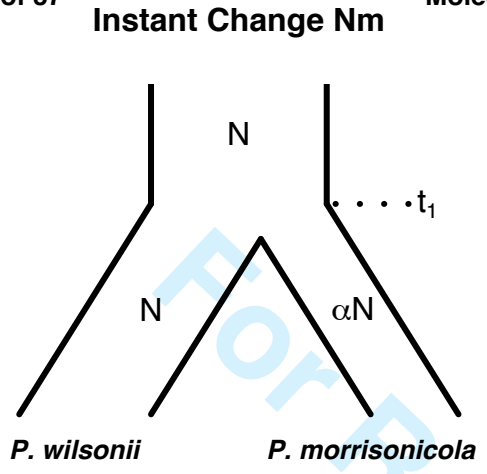

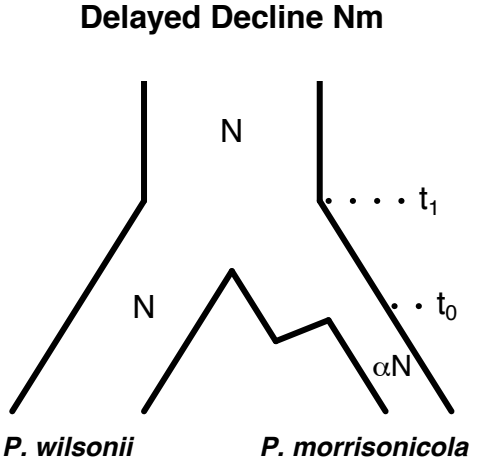

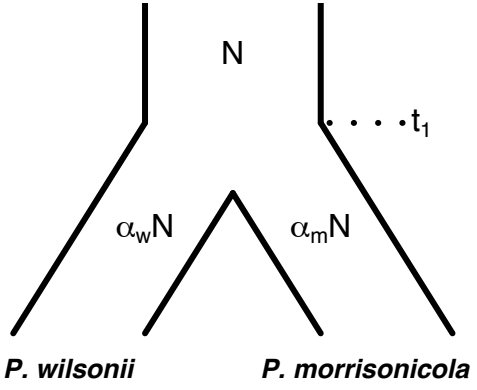

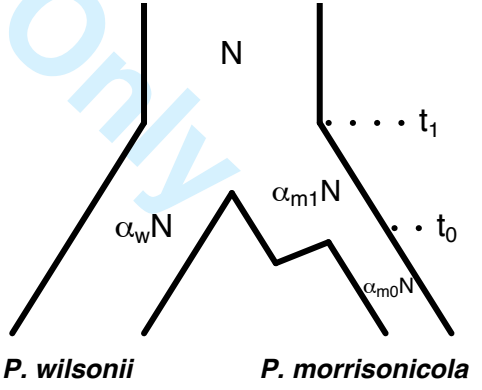

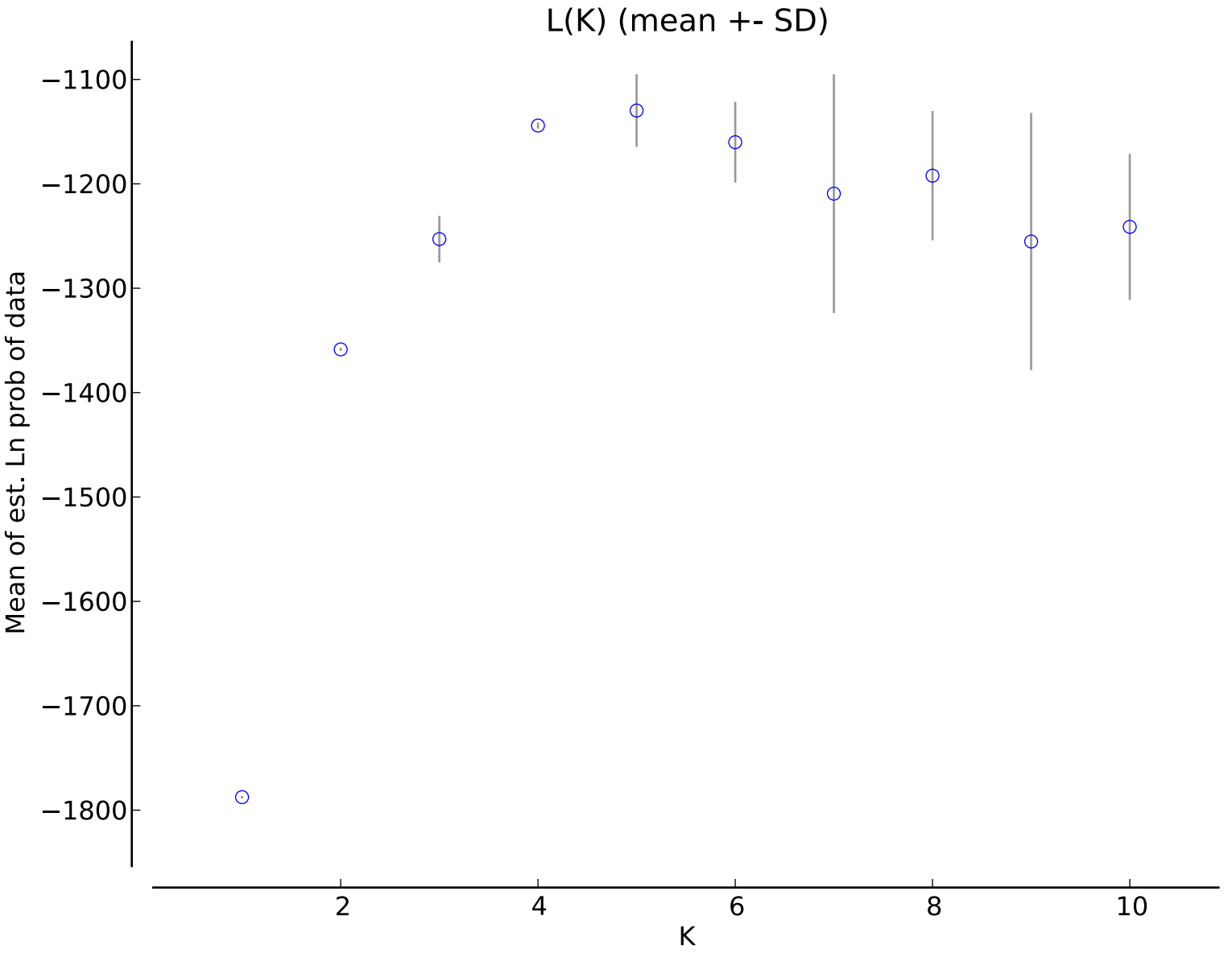
L(K) (mean +- SD)
Mean of est. Ln prob of data
−1100
−1200
−1300
−1400
−1500
−1600
−1700
−1800
2
4
6
8
10
K

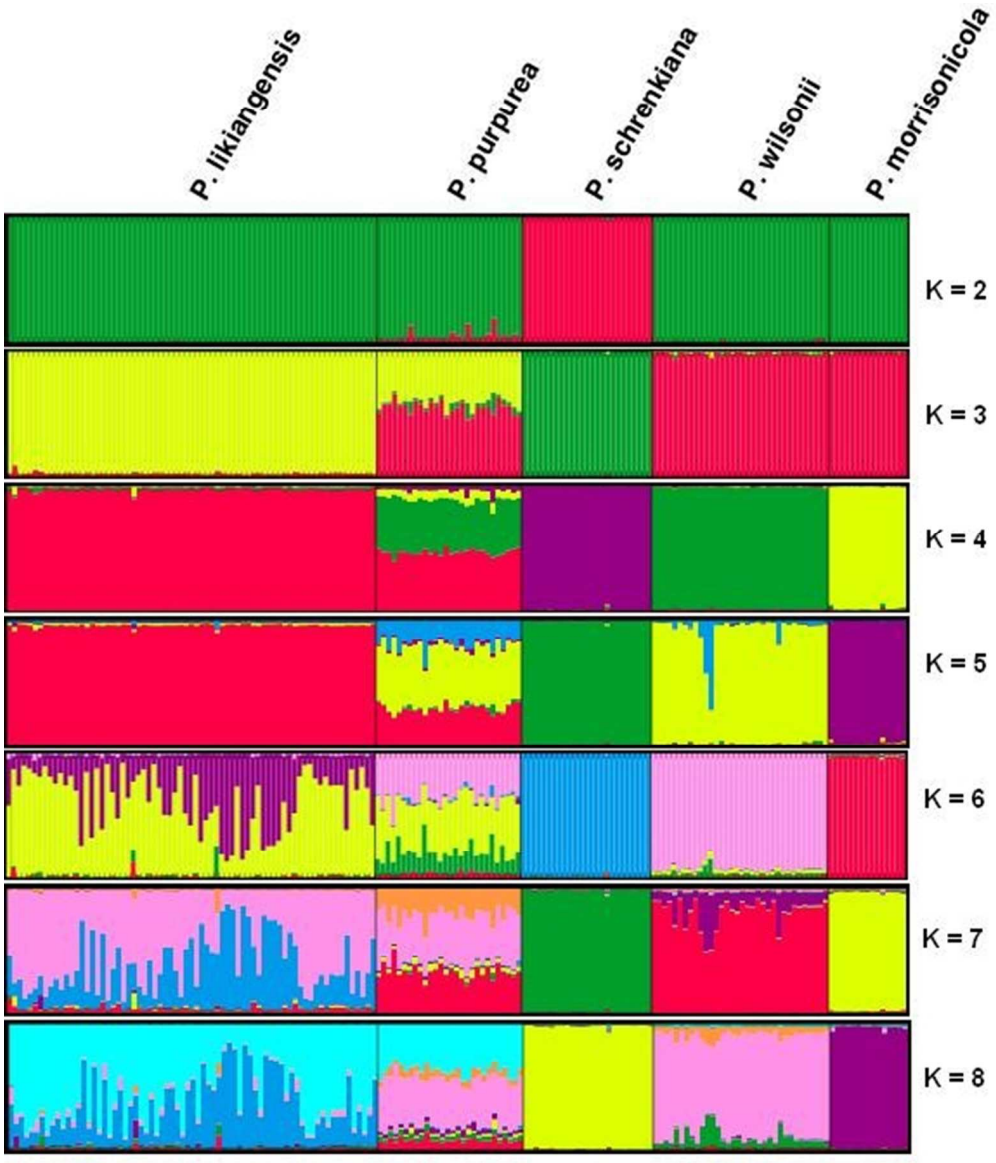

Figure 5: Ancestry estimates from Structure for K=2 through K=10 in the five species P. likiangensis (P.l.), P. purpurea (P.p.), P. schrenkiana (P.s.), P. wilsonii (P.w.) and P. morrisonicola (P.m.). Each K is represented by the Structure run that rendered the highest likelihood and shows the individual's estimated proportion of membership to each cluster.

97x113mm (150 x 150 DPI)

Table 1: Summary statistics per locus where n is the number of individuals, L is the length and S is the number of segregating sites. The statistics given are Watterson's θ (θ_W), the average number of pairwise nucleotide differences (π), Fay & Wu's θ (θ_H), Tajima's D (D), Fay & Wu's non-normalized H (H), Zeng's normalized H (Z) and the haplotypic diversity (He). For Tajima's D (D) and Fay & Wu's H (H) * indicates loci that deviate significantly from the standard neutral model without recombination.

Locus	n	L	S	θ_W	π	θ_H	D	H	Z	He
4cl	8	604	8	0.00511	0.00361	0.01484	-1.4213	-6.7857*	-3.6674	0.75
GI2	9	1590	0	0	0	0	-	-	-	0
GI4	10	985	0	0	0	0	-	-	-	0
GI6	14	1215	0	0	0	0	-	-	-	0
PCH	10	605	1	0.00058	0.00077	0.00033	0.8198	0.2667	0.5826	0.4667
SE1107	12	426	0	0	0	0	-	-	-	0
SE1390	11	551	7	0.00444	0.00629	0.00784	1.6842	-0.8364	-0.5199	0.7091
SE1464	15	419	0	0	0	0	-	-	-	0
SE6	15	445	1	0.00069	0.00094	0.00034	0.7421	0.2667	0.6112	0.419
ebs	8	785	0	0	0	0	-	-	-	0
m002	9	518	1	0.00072	0.00076	0.00267	0.1565	-0.9722	-2.0986	0.3889
sb16	13	804	9	0.00362	0.00519	0.00959	1.7028	-3.5256	-1.8449	0.4615
sb29	13	515	0	0	0	0	-	-	-	0
sb62	13	540	2	0.00119	0.00142	0.00043	0.5437	0.5385	0.8062	0.3846
SE1427	12	468	8	0.00566	0.00285	0.02745	-1.9834*	-11.5152*	-6.5351	0.1667
Average	-	698	-	0.00147	0.00146	0.00423	0.2805	-2.8204	-1.5832	0.2498

Table 2: Mode, 5% and 95% condence intervals of the posterior densities of the two combined MIMAR runs on the split model between *P. wilsonii* and *P. morrisonicola*. The parameters are population mutation rate in *P. wilsonii* (θ_1), *P. morrisonicola* ($\theta 2$) and the ancestral population (θ_A), symmetrical migration rate (M) and split time in generations (T_{gen}).

	θ_1	θ_2	θ_A	M	T_{gen}
Mode	0.005	0.0005	0.0008	0.35	160,000
5%	0.004	0.0003	0.0002	0.15	110,000
95%	0.006	0.001	0.004	0.61	220,000

Table 3: Bayes factors and model probabilities (in bold) amongst four competing within-species demographic scenarios. Bayes factors are calculated as the ratio of the marginal likelihoods of the two models under comparison: $p(y|M_1)/p(y|M_0)$.

		M_0			
		Constant Ne	Bottleneck	Decline	Structure
M_1	Constant Ne	**0.1413**	0.2384	0.1148	1.0601
	Bottleneck	4.1948	**0.1993**	0.675	1.8329
	Decline	8.7087	1.4814	**0.5241**	4.2647
	Structure	0.9433	0.5456	0.2345	**0.1353**

Table 4: Bayes factors and model probabilities (in bold) amongst four competing between-species demographic scenarios. Bayes factors are calculated as the ratio of the marginal likelihoods of the two models under comparison: $p(y|M_1)/p(y|M_0)$.

		M_0			
		IC_m	D_m	IC_{mw}	$IC_{mw}+D_m$
M_1	IC_m	**0.1828**	0.4276	1.4691	0.8051
	D_m	2.3389	**0.4512**	3.6512	1.805
	IC_{mw}	0.6807	0.2739	**0.1285**	0.5209
	$IC_{mw}+D_m$	1.2422	0.554	1.9197	**0.2375**

Table 5: The effective population size and timing of demographic events for the within-species (ABC_W) and between-species (ABC_B) ABC analyses. The effective population sizes for the ancestral (N_1) and present day (N_0) populations are calculated using a mutation rate of 2.5×10^{-8}. The time of divergence (T_1) and of the population decline (T_0) years are calculated assuming a generation of 25 years.

			Generations		Years	
	N_1	N_0	T_1	T_0	T_1	T_0
ABC_W	123841	1783	-	10729	-	268236
ABC_B	43737	4242	45056	14944	1126407	373598

Table 6: The power and the false positive rate (FPR) for each model for a dataset with the same number of samples and loci as that used in the study. Power is defined as the proportion of simulated datasets that *correctly* reject (Bayes factor ≥ 3) the alternative model in favor of the decline mode. The FPR is defined as the proportion of simulated datasets for which the alternative model is *incorrectly* rejected (simulated Bayes factor ≥ 3 or $\geq$ the observed Bayes factor) in favor of the decline model. The Bayes factors for the observed data, calculated for the given model against the decline model, are given in parentheses.

	Constant Ne (8.71)	Bottleneck (1.48)	Structure (4.27)
Power	0.81	0.3	0.95
$FPR_{\geq 3}$	0.07	0.01	0
$FPR_{\geq obs}$	0	0.12	0